Comparison of Rotor Wake Identification and Characterization Methods for the Analysis of Wake Dynamics and Evolution

E. W. Quon, P. Doubrawa, and M. Debnath
National Renewable Energy Laboratory, Golden, CO, USA
E-mail: Eliot.Quon@nrel.gov

Abstract.
Optimal wind power plant design requires understanding of wind turbine wake physics and validation of engineering wake models under wake-controlled operating conditions. In this work, we have developed and investigated several different wake identification and characterization methods for analyzing wake evolution and dynamics. The accuracy and robustness of these methods, based on Gaussian function fitting and adaptive contour identification, have been assessed by application to a large-eddy simulation data set. A new contour-based method based on downstream momentum deficit has been considered. Uncertainties arising from wake-identification errors result in characterizations of the wake expansion, recovery, and meandering motion that differ by 19% of the rotor area, 4% of the freestream, and 15% rotor diameter, respectively.

1. Introduction

Modern wind plant design leverages understanding of wake physics to increase energy capture and reduce structural loads, thereby reducing the cost of energy. Wake management strategies, such as wake steering, have the potential to achieve such goals [11] and have been evaluated with simulations [11, 19] and demonstrated with subscale and utility-scale experiments [5, 10]. The development and implementation of wake steering and other wind power plant control and design innovations rely on a quantifiable understanding of wind turbine wake behavior. This quantification is aided by algorithms that identify individual wakes in a measured or simulated flow field, characterizing their center and edges in dynamic and steady-state frameworks.

Wake identification and characterization can be a difficult task because of the turbulent atmospheric conditions in which the wakes are embedded (e.g., intermittent low-speed eddies in the flow could lead to false positives in wake identification) and limited flow information in the case of field measurements. As a consequence, over the years, researchers have independently developed various distinct approaches to tracking wakes that are based on their individual needs and resources. This lack of coordination in wake analyses can lead to higher uncertainty in results and engender confusion among researchers regarding which methodology should be applied under which conditions. Here, we address these issues by presenting a new open-source, Python-based library of wake tracking algorithms called the Simulated And Measured Wake Identification and CHaracterization ToolBox (SAMWICH Box) [17]. The algorithms implemented within SAMWICH Box are based on previously proposed methods described in published literature.


Content from this work may be used under the terms of the Creative Commons Attribution 3.0 licence. Any further distribution of this work must maintain attribution to the author(s) and the title of the work, journal citation and DOI.
Published under licence by IOP Publishing Ltd

The various methods can be tested on model data (e.g., Reynolds-Averaged Navier-Stokes or large-eddy simulations) or field measurements to demonstrate their merits and shortcomings and to quantify the uncertainty that can be expected from wake data analysis alone due to the choice of wake-tracking algorithm.

2. Wake Identification and Characterization Methods

Hereinafter, "wake identification" refers to the identification of the wake edges and/or centers in a simulated or measured flow field. Given turbulent flow conditions, the definition of a wake edge is rarely straightforward due to the nature of the flow as well as data availability. The following step in our analysis, "wake characterization," makes use of the identified center and edges to diagnose wake shape and size, trajectory, recovery, and meandering. For x, y, and z coordinates aligned with the streamwise, cross-stream, and vertical directions, the wake identification is often done in planes: horizontal (along x and y) planes, at or near the turbine hub height; or vertical transverse planes that slice through the wake along the lateral and vertical directions (i.e., y and z). Here, we focus on the latter so that vertical meandering and deflection will not affect the diagnosed wake characteristics (as opposed to a horizontal plane, which will slice the wake at different heights depending on its vertical deflection and motion, or not intersect the wake at all [1]). In the following section, wake-identification approaches from published literature are reviewed. Four of these approaches are considered in this study, as described in Sections 2.1 to 2.3 and summarized in Table 1.

2.1. Function-Based Wake-Identification Methods

The first approach to wake identification has origins in wake modeling. At a given downstream distance, canonical wakes are typically modeled with a Gaussian function (double Gaussian in the near wake [1, 15] and single Gaussian in the far wake [11, 18]) whose parameters dictate the wake shape and orientation. These functions can be fit to measured and simulated flow fields to estimate the wake center and approximate its size (i.e., the Gaussian width σ) or area. These function-based approaches are straightforward to implement and computationally inexpensive. They can also be applied to both horizontal (one-dimensional Gaussian fit) and transverse (one- and two-dimensional Gaussian fits) data and can accommodate wakes that lie partially outside of the sampled region. However, there is significant sensitivity to the first guess for the functional parameters and, especially in cases with irregularly shaped wakes, a fit may not be found. In the present study, both one-dimensional ("1D Gaussian") based on the Bastankhah model [3] and two-dimensional ("2D Gaussian") Gaussian fit methods are considered. The 2D Gaussian fit implemented in SAMWICH Box solves an optimization problem for the wake position, shape (σ_y, σ_z), and rotation (to account for skewed wakes).

2.2. Threshold-Based Wake-Identification Methods

Another straightforward approach is to specify a threshold or cut-off value to identify regions of the flow field as being inside or outside of the rotor wake. This cut off can be specified as a function of the inflow velocity (e.g., 95% of the freestream wind speed [14, 9]) or wake velocity (e.g., 20%–50% of the velocity deficit [4] or the corresponding 95% confidence interval if the wake distribution were Gaussian [8]). Once the wake edges are identified, the wake center may be specified as the average of the wake edges [14, 9] or the velocity-deficit-weighted average (also referred to as the velocity-deficit "center of gravity") in the interior of the wake [16, 8, 13]. This approach is also applicable to horizontal and transverse data, but may misrepresent the wake size and location if the wake lies partially outside of the sampled region. In addition, the threshold value can vary with downstream distance depending on the rate of wake recovery which, in turn, is susceptible to the ambient turbulence level. Although this is a simple method to implement, some researchers have reported a high rejection rate for detected wakes [9].

Table 1. Summary of wake identification methods and the associated inputs, outputs, and properties.

Method	Inputs	Center Detection	Edge Detection	Shape Detection
1D Gaussian, Fixed σ	ref. length	approx.	approx.	n/a
1D Gaussian, Bastankhah [3]	ref. thrust, TI	approx.	approx.	n/a
2D Gaussian fit	n/a	approx.	approx.	approx.
Constant area [6, 12]	ref. area	weighted	exact	exact
Constant momentum deficit	ref. thrust	weighted	exact	exact
Minimum power [18]	n/a	approx.	n/a	n/a

2.3. Contour-Based Wake-Identification Methods

A third approach is based on identifying velocity (or velocity deficit) isocontours in the flow data, where the contours conveniently serve as boundaries for wake regions. This may be thought of as an adaptive threshold approach. Through evaluating the bounded area or functions of velocity—for example, the momentum or energy flux through the enclosed region—wakes may be discriminated by comparison against a predefined reference value. A wake may be identified by contours in the transverse plane that have a constant area (e.g., the rotor area [6, 12]). Or, a more computationally demanding approach is to identify the wake based on the flux through the velocity contours with the comparison value chosen from fundamental physical quantities such as mass flow or momentum flux (similar to the approach in [18]). Although the physical basis of these contour-based approaches can offer increased robustness, they are only applicable to transverse sampled data. Similar to the threshold-based approaches, the contour-based methods require an additional step to determine the wake location and size. Here, two contour-based methods are considered: "constant area" and "constant momentum deficit," with the wake "center" defined as the velocity-deficit-weighted center of mass within the identified contour region. For the constant momentum deficit approach, the reference momentum flux is determined from the rotor thrust.

2.4. Wake Characterization

The four wake-identification methods considered herein produce instantaneous estimates of the wake outline and center at each distance downstream (as exemplified in Fig. 1). These sequential wake snapshots highlight some of the challenges of wake identification. First, the shape of the wake is highly irregular, and the identified shape may vary depending on the identification method. Second, the interior of the wake may not be well defined in that it does not necessarily have a well-defined center (in terms of local maxima in velocity deficit) or pronounced velocity deficit to distinguish it from the freestream. Third, the wake size, position, and strength (in terms of velocity deficit) may rapidly change because of the background turbulence.

After a wake identification algorithm has been applied, the resulting wake trajectory is not guaranteed to be free from spurious wake center identifications or missing wakes. This necessitates additional quality-control measures. Common filtering approaches involve taking the average or median over a sliding window of fixed size. In a preliminary study, we manually identified reference wake trajectories for select downstream distances and analysis periods, to which we compared the filtered wake trajectories obtained from our algorithms (Fig. 2). Motivated by work in the field of image processing, we applied one- and two-stage moving-median filters with varying window sizes [2] to mitigate the effect of discontinuities in the wake-position history while preserving local extrema. We found that for wakes in a neutrally stable atmosphere, any sliding window larger than 3–5 s had a tendency to overly smooth the wake

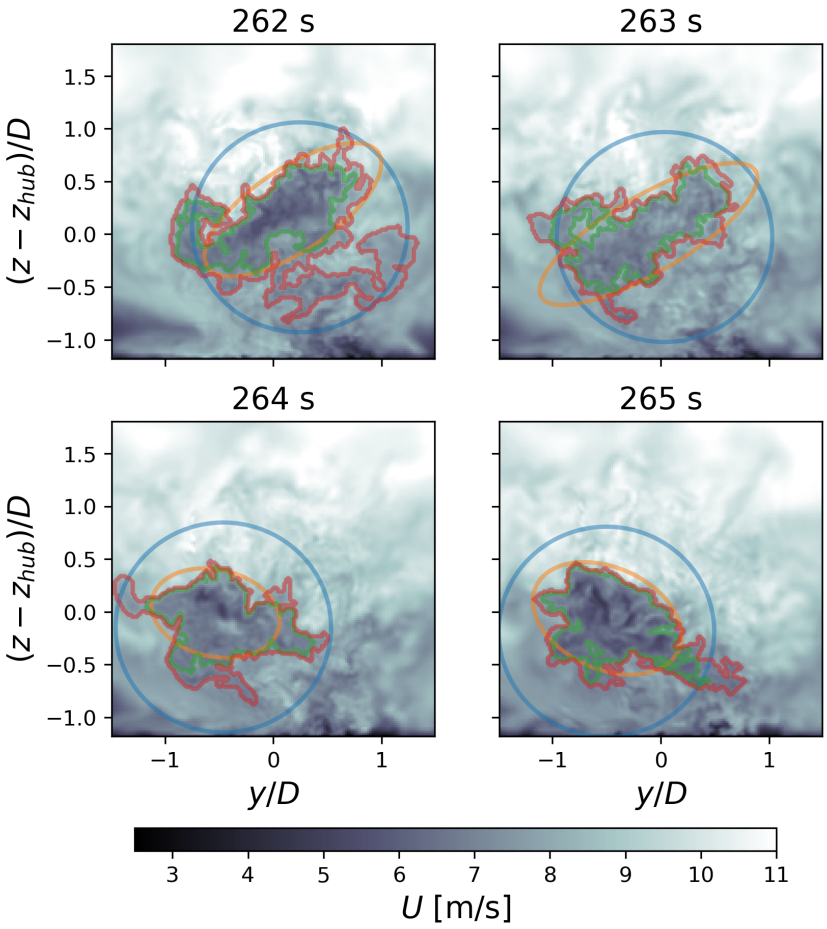

Figure 1. Rotor-wake cross sections at 6 rotor diameters downstream, at four consecutive instances in time. Outlines are shown of the wakes detected by the 1D Gaussian (blue), 2D Gaussian (orange), constant-area contours (green), and constant momentum deficit contours (red).

signal, thereby reducing the amount of meandering motion and increasing error relative to our reference trajectory. Therefore, for the remainder of this work, we apply only a 3-s moving-median filter.

From the time history of the wake position, other quantities can be diagnosed to analyze the mean and dynamic behavior of the wake. The analysis presented in Section 4 considers: (i) wake expansion (downstream evolution of the area inside a predetermined velocity deficit contour, considering temporally averaged flow); (ii) wake recovery (downstream evolution of the maximum velocity deficit, considering temporally averaged flow); and (iii) wake meandering (the standard deviation of wake-center position over time). Because four wake identification methods are considered, four sets of wake diagnostics are also obtained. The differences between these diagnostics are then used to estimate the level of uncertainty that can be expected in wake studies as it pertains to data-analysis choices.

3. Data

The wake identification and characterization methods described in Section 2 are applied to a large-eddy simulation (LES) data set of a single wake under near-neutral stratification. The

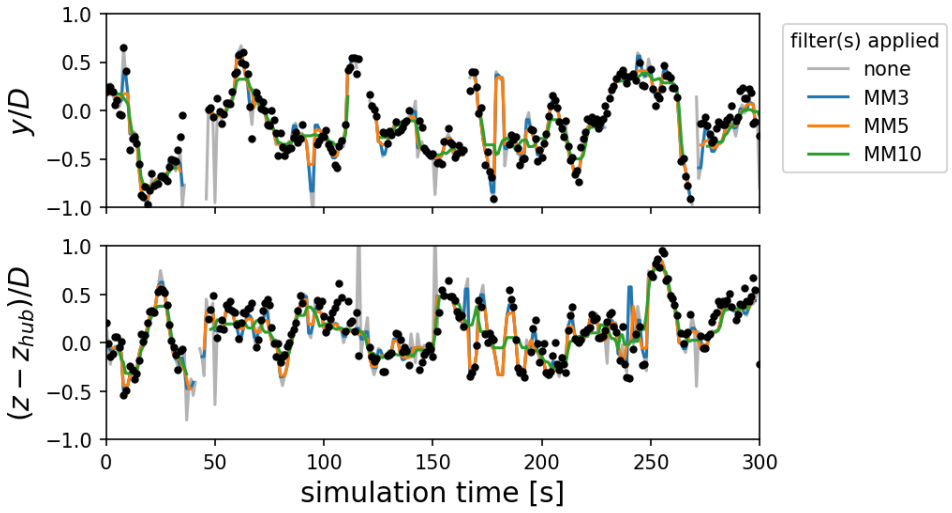

Figure 2. Time history of the rotor wake position detected by a 2D Gaussian fit, with moving median (MM) filters of various window sizes applied. Symbols indicate the "true" wake center as determined by an analyst.

simulation is performed with the National Renewable Energy Laboratory (NREL) Simulator fOr Wind Farm Applications (SOWFA) tool. The workflow involves first simulating only the atmospheric boundary layer (without a wind turbine) on a periodic domain. The flow field generated with this precursor simulation is then used as initial and boundary conditions to a second simulation on a finite domain that contains the wind turbine.

The atmospheric conditions being simulated are based on measurements obtained at the U.S. Department of Energy (DOE) Scaled Wind Farm Technology (SWiFT) facility in Lubbock, Texas, and used to define benchmarks for model validation [7]. The target mean hub-height wind speed and turbulence intensity are 8.7 m/s and 10.7%, with a vertical shear that corresponds to a power-law exponent of 0.14. To obtain this inflow, the following parameters were prescribed to the model: capping inversion height = 750 m; capping inversion thickness = 100 m; lower boundary temperature = 314.4 K; roughness length = 0.0145 m; latitude = 33.60795°. The mesh was defined to extend 3.2-km axially (along x) and laterally (along y), and 1-km vertically (along z). For the precursor atmospheric simulation, the grid spacing was set to 8 m in x and y and varied between 5 m and 10 m in z (with higher resolution close to the surface). The simulated flow matched the hub-height wind speed, with turbulence intensity and shear exponent of 9.9% and 0.16, respectively.

The wind turbine being simulated is a modified Vestas V27 with a hub height of 32.1 m and rotor diameter (D) of 27 m (with no yaw offset). The turbine was modeled with actuator lines and the mesh was refined between -6D and 10D around the turbine down to a grid spacing of 0.5 m. The simulation was run for a total of 30 minutes (plus spin up) and the flow field was sampled upstream (at -2.5D) and in the wake (between 2D and 8D, in 1D increments) every second on transverse slices parallel to the rotor. These transverse snapshots of three-dimensional flow were then used as input to the various wake identification algorithms.

4. Results & Discussion

To assess the effectiveness of and quantify the uncertainty inherent in the different wake-tracking approaches, we consider the evolution and dynamics of the rotor wake in meandering and fixed frames of reference (MFoR and FFoR, respectively). Time-averaged quantities within the

MFoR more closely resemble canonical wakes, thereby facilitating analysis of wake expansion and recovery. Moreover, because the transformation to the MFoR requires knowledge of the wake center, the expansion and recovery characteristics may be used to assess the goodness of the wake identification provided by SAMWICH Box. In the FFoR, we consider the unsteady motions of the wake to characterize the meandering behavior of the wake.

4.1. Wake Expansion

Figure 3 illustrates wake evolution in the MFoR with downstream distance. The background turbulence has been averaged out along with irregularities in the wake shape. What remain are a well-defined velocity deficit region and a small apparent speed-up region below the rotor in the near wake, both of which diminish noticeably with downstream distance. The speed-up is exaggerated by interpolating to the MFoR when the wake is near to the ground. Because extrapolation is not performed, there are fewer points over which the time average is taken.

To highlight differences between the identified wakes, we extract contours from the wake velocity field at 95%, 90%, and 70% of the hub-height freestream velocity (i.e., the red contours in Fig. 3). From these contours, we calculate the enclosed area to assess the expansion of the wake with downstream distance (Fig. 4). The inner-most wake region containing the greatest velocity deficit ($U_{wake} = 0.7U_{ref}$) decreases in size linearly, vanishing for all methods by $x \approx 5D$. In comparison, the outer edges of the wake suggest different rates at which energy is entrained from the freestream (as indicated by $U_{wake} = 0.9U_{ref}$), with the velocity deficit decaying more rapidly near the edges of the wake when performing identification with the 2D Gaussian fit. This is especially true after the inner wake has mixed out (i.e., for $x > 5D$). When considering the outermost contour ($U_{wake} = 0.95U_{ref}$), there is consensus across methods that the wake stops expanding between 6–7D downstream; the exception is the 1D Gaussian wake, which appears to predict a wake with unchecked expansion. This is likely a consequence of the 1D model being unable to adequately represent more irregular wakes and because the modeled wake size and strength are invariant in time (e.g., see Fig. 1), all of which introduce errors in the wake position that translate into excessive diffusion in the MFoR. From the $0.95U_{ref}$ contour, the wakes differ both in maximum area (between the constant-area and constant-momentum-deficit contour approaches) by $0.19A$ (where A is the rotor area) and in the downstream location at which the maximum occurs (6–7D).

4.2. Wake Recovery

The MFoR data in Fig. 3 are also used to assess the rate at which the wake recovers to freestream conditions (Fig. 5). Although all methods once more agree near the rotor (e.g., $x = 2D$), the differences in the maximum velocity deficit increase with downstream distance. In the near wake, the strength of the wake based on the contour-based approaches is similar to the predictions of the 1D Gaussian. However, the 1D Gaussian predictions overpredict wake diffusion as noted in the previous section, thus underpredicting the strength of the wake in the far wake. In the far wake, the contour-based approaches predict a wake that is closer in strength to the 2D Gaussian wake. Between all methods, however, the velocity deficits differ at most by only 0.33 m/s or 4%.

4.3. Wake Meandering

We estimate the lateral and vertical motions of the wake from the time histories of the detected wake positions. Figure 6 shows the standard deviation of the wake position at distances up to 8 rotor diameters downstream. Good agreement between all wake identification algorithms is observed in the near wake with lateral and vertical fluctuations in wake position of $0.12D$ and $0.08D$, respectively, at $2D$ from the rotor. The magnitude of the wake motions increases linearly with lateral motions being consistently 50% larger than the vertical motions. However, in the far wake, greater variability has been observed between methods. At $8D$ downstream,

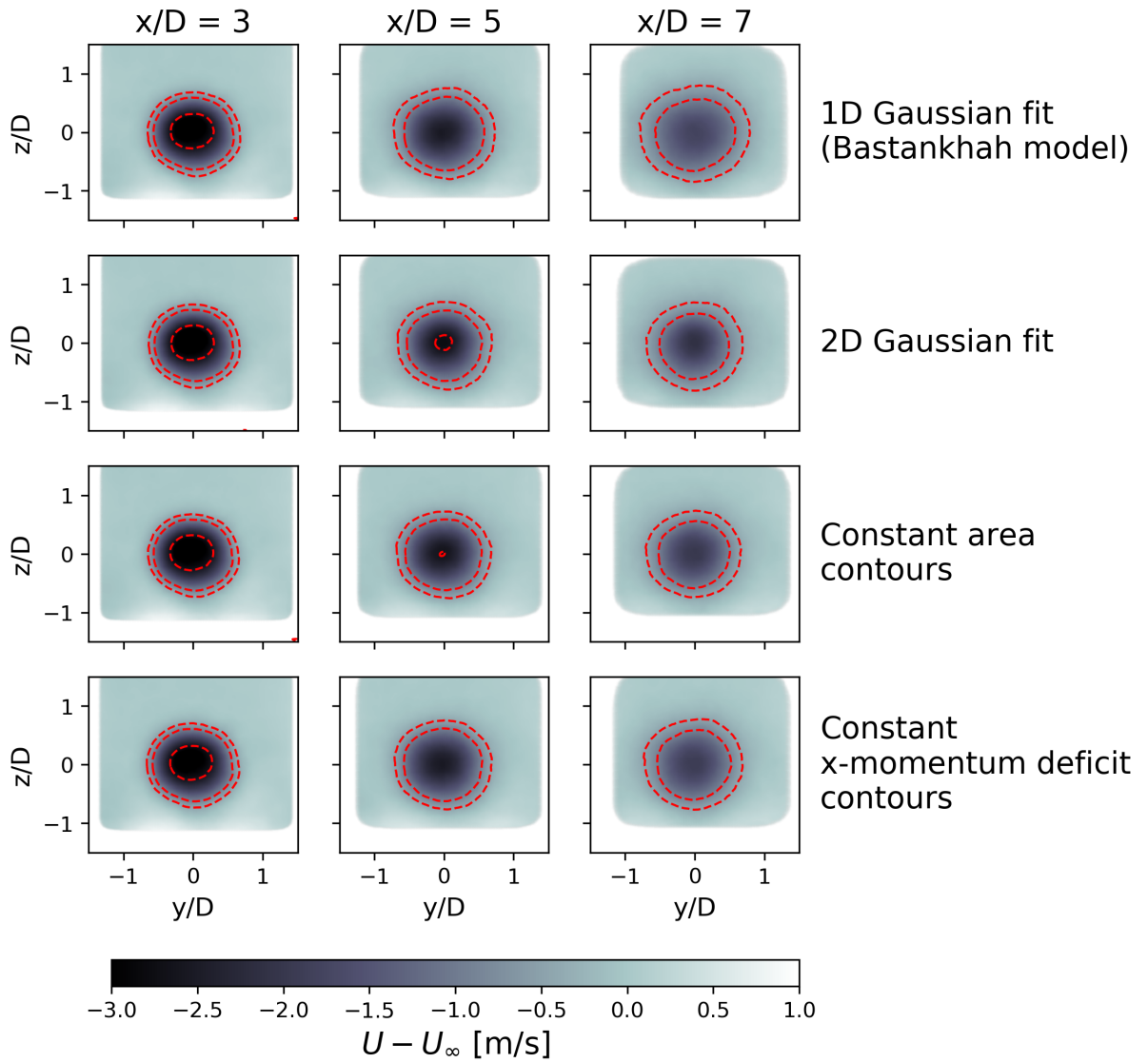

Figure 3. Time-averaged wakes in a meandering frame of reference for four different wake-tracking methods. Dashed red contours indicate where the wake velocity is 95%, 90%, and 70% of the freestream velocity (U_∞), in order of decreasing radial distance from the wake center; note that the $0.7U_{ref}$ contour only exists near to the rotor.

the estimated standard deviation in position ranges more than $0.15D$ in the horizontal direction and more than $0.08D$ in the vertical. We also observe that the estimated meandering motion is higher for Gaussian-function fitting than the contour approaches.

5. Conclusions

To assess the degree to which upstream and downstream turbines interact within a wind power plant, and the extent to which wake control strategies may be utilized, we have analyzed the evolution and dynamics of LES-simulated wakes. The ability of a wake-identification algorithm to reliably locate the center of a wake given an instantaneous cross section dictates the accuracy of the calculated expansion, recovery, and meandering characteristics. To the authors'

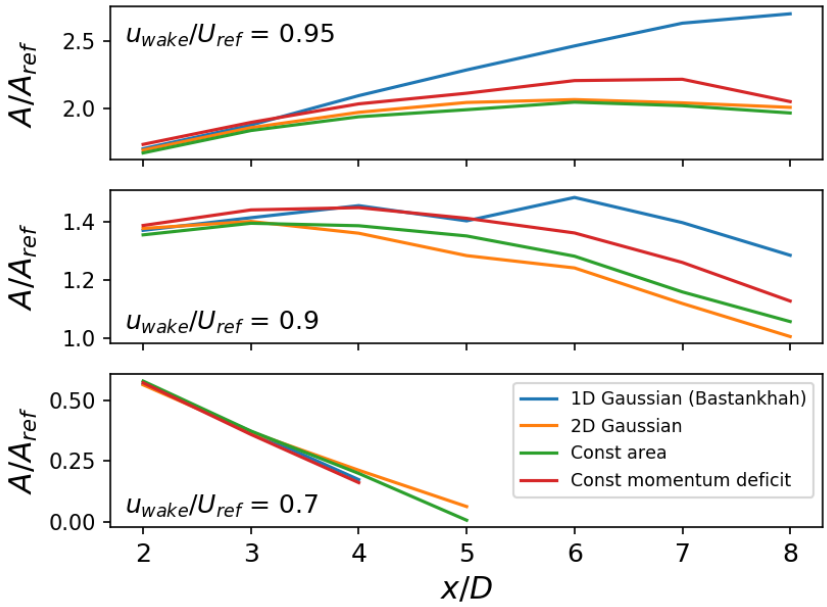

Figure 4. Evolution of the time-averaged wake area (in a meandering frame of reference) with downstream distance as characterized by velocity contours at 95%, 90%, and 70% of the freestream velocity.

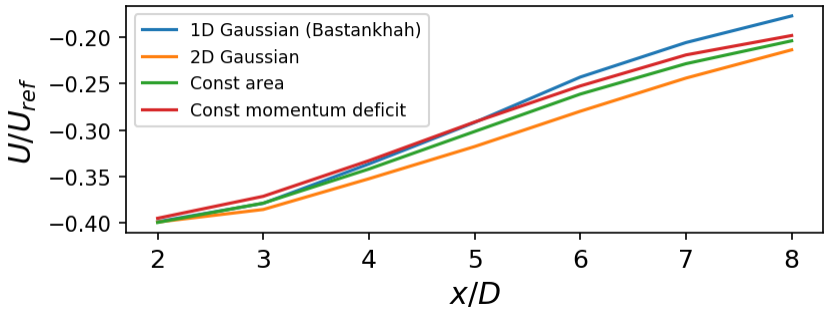

Figure 5. Evolution of the time-averaged maximum velocity deficit (in a meandering frame of reference) with downstream distance.

knowledge, there has not been a previous study directly comparing wake tracking methods applied to the same data set. The approach we have followed is to apply a set of baseline wake-identification parameters to algorithms implemented within the open-source Python library, SAMWICH Box, and then use a moving-median filter for quality control—we do not in general expect the identification algorithms to consistently outperform a human analyst but instead aim to quantify the uncertainties that arise from different choices of wake identification and characterization methods.

Although computationally efficient and simple, the 1D Gaussian appears to be inadequate as a template for wake identification from instantaneous snapshots of wake cross sections. Diffusive errors have been noted in the wake evolution, and lateral wake meandering may be overpredicted by up to 15% of the rotor diameter. Such characterization errors may negatively impact the calibration and validation of engineering and midfidelity models. It may be possible to improve

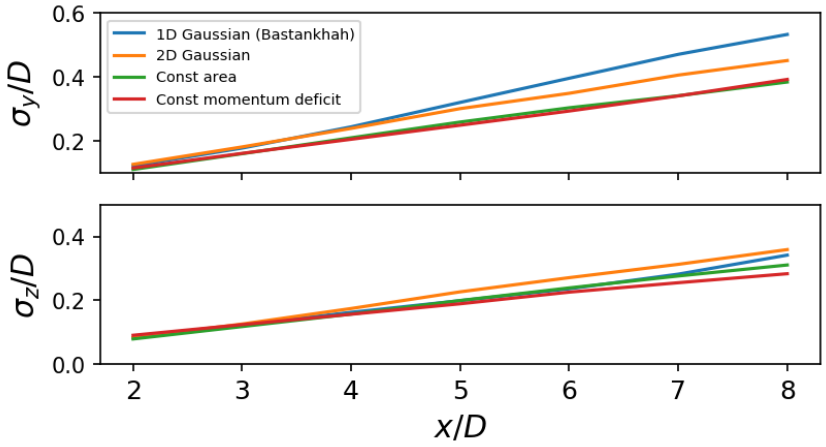

Figure 6. Standard deviation of the lateral (top subfigure) and vertical (bottom subfigure) wake positions as a function of downstream distance.

this approach, for example, by improving the wake growth model for the simulated set of conditions.

Between the 2D Gaussian fit and contour-based methods, differences have also been noted. For example, the 2D Gaussian may predict a slightly stronger velocity deficit, differing by up to 4% of the freestream velocity. Larger lateral wake motions were also predicted compared to the contour-based methods. Between the constant-area and constant-momentum-deficit approaches, the constant momentum-deficit naturally allows the algorithm to adapt and account for wake expansion downstream. Therefore, it is not surprising that the constant-area approach underpredicts the wake area by 19% in the far wake.

The current work considers only a single set of conditions at near-neutral atmospheric stability. Under convective conditions, the wakes should be less well-defined because of stronger turbulent mixing. Therefore, we expect that wake identification and characterization of the unstable near wake would be comparable to the neutral far wake. Stable conditions may offer additional challenges in the presence of significant veer or yaw misalignment because of deformation of the wake. This should be automatically accounted for by the contour-based approaches but not necessarily by the 2D Gaussian (in the misaligned case in which wake curling is typically observed) or the 1D Gaussian (under both non-neutral conditions). Future work may include more detailed analysis of instantaneous wakes and evaluation of spatial filtering techniques to reduce noise (i.e., turbulence fluctuations) from the sampled wake.

Acknowledgements

This work was authored by the National Renewable Energy Laboratory, operated by Alliance for Sustainable Energy, LLC, for the U.S. Department of Energy (DOE) under Contract No. DE-AC36-08GO28308. Funding provided by the U.S. Department of Energy Office of Energy Efficiency and Renewable Energy Wind Energy Technologies Office. The views expressed in the article do not necessarily represent the views of the DOE or the U.S. Government. The U.S. Government retains and the publisher, by accepting the article for publication, acknowledges that the U.S. Government retains a nonexclusive, paid-up, irrevocable, worldwide license to publish or reproduce the published form of this work, or allow others to do so, for U.S. Government purposes.

References

[1] Matthew L. Aitken, Robert M. Banta, Yelena L. Pichugina, and Julie K. Lundquist. Quantifying Wind Turbine Wake Characteristics from Scanning Remote Sensor Data. *Journal of Atmospheric and Oceanic*

Technology, 31(4):765–787, January 2014.

[2] Ery Arias-Castro and David L. Donoho. Does median filtering truly preserve edges better than linear filtering? *The Annals of Statistics*, 37(3):1172–1206, June 2009.

[3] Majid Bastankhah and Fernando Porté-Agel. A new analytical model for wind-turbine wakes. *Renewable Energy*, 70:116–123, October 2014.

[4] David Bastine, Björn Witha, Matthias Wächter, and Joachim Peinke. Towards a Simplified DynamicWake Model Using POD Analysis. *Energies*, 8(2):895–920, February 2015.

[5] F. Campagnolo, V. Petrović, C. L. Bottasso, and A. Croce. Wind tunnel testing of wake control strategies. In *2016 American Control Conference (ACC)*, pages 513–518, July 2016.

[6] M. Churchfield, Q. Wang, A. Scholbrock, T. Herges, T. Mikkelsen, and M. Sjöholm. Using High-Fidelity Computational Fluid Dynamics to Help Design a Wind Turbine Wake Measurement Experiment. *Journal of Physics: Conference Series*, 753:032009, September 2016.

[7] P. Doubrawa, M. Debnath, P. J. Moriarty, E. Branlard, T. G. Herges, D. C. Maniaci, and B. Naughton. Benchmarks for Model Validation based on LiDAR Wake Measurements. *Journal of Physics: Conference Series*, 1256:012024, July 2019.

[8] Paula Doubrawa, Rebecca J. Barthelmie, Hui Wang, S. C. Pryor, and Matthew J. Churchfield. Wind Turbine Wake Characterization from Temporally Disjunct 3-D Measurements. *Remote Sensing*, 8(11):939, November 2016.

[9] G. España, S. Aubrun, S. Loyer, and P. Devinant. Spatial study of the wake meandering using modelled wind turbines in a wind tunnel. *Wind Energy*, 14(7):923–937, 2011.

[10] Paul Fleming, Jennifer Annoni, Andrew Scholbrock, Eliot Quon, Scott Dana, Scott Schreck, Steffen Raach, Florian Haizmann, and David Schlipf. Full-Scale Field Test of Wake Steering. *Journal of Physics: Conference Series*, 854:012013, May 2017.

[11] Paul A. Fleming, Pieter M. O. Gebraad, Sang Lee, Jan-Willem van Wingerden, Kathryn Johnson, Matt Churchfield, John Michalakes, Philippe Spalart, and Patrick Moriarty. Evaluating techniques for redirecting turbine wakes using SOWFA. *Renewable Energy*, 70:211–218, October 2014.

[12] T. G. Herges, D. C. Maniaci, B. T. Naughton, T. Mikkelsen, and M. Sjöholm. High resolution wind turbine wake measurements with a scanning lidar. *Journal of Physics: Conference Series*, 854:012021, May 2017.

[13] Michael F. Howland, Juliaan Bossuyt, Luis A. Martínez-Tossas, Johan Meyers, and Charles Meneveau. Wake structure in actuator disk models of wind turbines in yaw under uniform inflow conditions. *Journal of Renewable and Sustainable Energy*, 8(4):043301, July 2016.

[14] Ángel Jiménez, Antonio Crespo, and Emilio Migoya. Application of a LES technique to characterize the wake deflection of a wind turbine in yaw. *Wind Energy*, 13(6):559–572, 2010.

[15] Aidan Keane, Pablo E. Olmos Aguirre, Hannah Ferchland, Peter Clive, and Daniel Gallacher. An analytical model for a full wind turbine wake. *Journal of Physics: Conference Series*, 753:032039, September 2016.

[16] Rolf-Erik Keck, Martin de Maré, Matthew J. Churchfield, Sang Lee, Gunner Larsen, and Helge Aagaard Madsen. On atmospheric stability in the dynamic wake meandering model. *Wind Energy*, 17(11):1689–1710, November 2014.

[17] Eliot Quon. *SAMWICH Box: A Python-Based Toolbox for Simulated And Measured Wake Identification and CHaracterization*. `https://github.com/ewquon/waketracking`.

[18] Lukas Vollmer, Gerald Steinfeld, Detlev Heinemann, and Martin Kühn. Estimating the wake deflection downstream of a wind turbine in different atmospheric stabilities: an LES study. *Wind Energy Science*, 1(2):129–141, September 2016.

[19] Jiangang Wang, Chengyu Wang, Filippo Campagnolo, and Carlo L. Bottasso. Wake behavior and control: comparison of LES simulations and wind tunnel measurements. *Wind Energy Science*, 4(1):71–88, January 2019.